

# Mice with altered KCNQ4 K<sup>+</sup> channels implicate sensory outer hair cells in human progressive deafness

Tatjana Kharkovets<sup>1</sup>, Karin Dedek<sup>1,4</sup>,  
Hannes Maier<sup>2</sup>, Michaela Schweizer<sup>1</sup>,  
Darina Khimich<sup>3</sup>, Régis Nouvian<sup>3</sup>,  
Vitya Vardanyan<sup>1</sup>, Rudolf Leuwer<sup>2</sup>,  
Tobias Moser<sup>3</sup> and  
Thomas J Jentsch<sup>1,\*</sup>

<sup>1</sup>Zentrum für Molekulare Neurobiologie, ZMNH, Universität Hamburg, Hamburg, Germany, <sup>2</sup>Department of Otolaryngology, Universitätsklinikum Hamburg-Eppendorf, Hamburg, Germany and <sup>3</sup>Department of Otolaryngology, Center for Molecular Physiology of the Brain, University of Göttingen, Göttingen, Germany

KCNQ4 is an M-type K<sup>+</sup> channel expressed in sensory hair cells of the inner ear and in the central auditory pathway. KCNQ4 mutations underlie human DFNA2 dominant progressive hearing loss. We now generated mice in which the *KCNQ4* gene was disrupted or carried a dominant negative DFNA2 mutation. Although KCNQ4 is strongly expressed in vestibular hair cells, vestibular function appeared normal. Auditory function was only slightly impaired initially. It then declined over several weeks in *Kcnq4*<sup>-/-</sup> mice and over several months in mice carrying the dominant negative allele. This progressive hearing loss was paralleled by a selective degeneration of outer hair cells (OHCs). KCNQ4 disruption abolished the *I<sub>K,n</sub>* current of OHCs. The ensuing depolarization of OHCs impaired sound amplification. Inner hair cells and their afferent synapses remained mostly intact. These cells were only slightly depolarized and showed near-normal presynaptic function. We conclude that the hearing loss in DFNA2 is predominantly caused by a slow degeneration of OHCs resulting from chronic depolarization.

*The EMBO Journal* (2006) 25, 642–652. doi:10.1038/sj.emboj.7600951; Published online 26 January 2006  
Subject Categories: neuroscience

Keywords: capacitance; channelopathy; KCNQ5; ribbon synapse; vestibular organ

## Introduction

Hearing loss is the most frequent inherited sensory defect in humans and increases dramatically with age (Petit *et al*, 2001). Inherited hearing loss may be syndromic (associated

with other abnormalities) or nonsyndromic. Nonsyndromic deafness may be inherited as X-linked, autosomal dominant or/and autosomal recessive traits. In general, autosomal recessive deafness has an early onset and is very severe, whereas autosomal dominant deafness often develops slowly over decades.

We had cloned KCNQ4 as a hitherto unknown member of the KCNQ K<sup>+</sup> channel family, have mapped its gene to the DFNA2 deafness locus and have identified *KCNQ4* mutations in patients with DFNA2 (Kubisch *et al*, 1999). These mutations suppressed currents of coexpressed wild-type (WT) subunits in a dominant negative manner. Like other KCNQ channels, in particular KCNQ2–KCNQ3 heteromers (Schroeder *et al*, 1998; Wang *et al*, 1998), KCNQ4 mediates M-type K<sup>+</sup> currents (Kubisch *et al*, 1999). M-currents may regulate neuronal excitability and are characterized by their modulation through neurotransmitters, their voltage dependence and their pharmacological profile (Jentsch, 2000). Most KCNQ proteins (KCNQ2 to KCNQ5) can form homo- and heteromeric channels. KCNQ3 is able to associate with all KCNQ proteins except for KCNQ1. The carboxy-terminal domain mediating subunit-specific interactions has been mapped (Schwake *et al*, 2003). KCNQ4 can form functional heteromers with KCNQ3 in heterologous expression systems (Kubisch *et al*, 1999), but it is unknown whether this occurs *in vivo*. In the inner ear, KCNQ4 mRNA was localized to outer hair cells (OHCs) of the organ of Corti (Kubisch *et al*, 1999). Immunocytochemistry revealed the presence of the KCNQ4 protein in plasma membranes of OHCs and type I vestibular hair cells (Kharkovets *et al*, 2000). In the first few days after birth, KCNQ4 was expressed in the entire basal and lateral membrane of OHCs (Boettger *et al*, 2002), but after the onset of hearing (P12–14), it localized exclusively to the basal pole. This localization suggested (Kharkovets *et al*, 2000) that KCNQ4 might serve to extrude K<sup>+</sup> ions that enter OHCs through apical mechanosensitive channels, which may be encoded by TrpA1 (Corey *et al*, 2004). After their exit from OHCs, K<sup>+</sup> ions are taken up by supporting cells, presumably using K–Cl cotransport (Boettger *et al*, 2002, 2003). KCNQ4 is also quite specifically expressed in several nuclei and tracts of the central auditory pathway in the brainstem (Kharkovets *et al*, 2000).

In order to understand the mechanism leading to DFNA2 deafness and to elucidate the role of KCNQ4 in hearing, we now generated a constitutive knockout (KO) of KCNQ4 and a knock-in (KI) of a dominant negative KCNQ4 mutation we had identified in DFNA2 patients (Kubisch *et al*, 1999). Our results show that deafness is due to a slow degeneration of cochlear OHCs. This degeneration is faster in the total KO than in animals heterozygous for the dominant negative mutation. Our study identifies the native K<sup>+</sup> currents that are mediated by KCNQ4 and provides animal models for human progressive deafness.

\*Corresponding author. Zentrum für Molekulare Neurobiologie, ZMNH, Universität Hamburg, Falkenried 94, Hamburg 20246, Germany.

Tel.: +49 40 42803 4741; Fax: +49 40 42803 4839;

E-mail: Jentsch@zmnh.uni-hamburg.de

<sup>4</sup>Present address: Carl-von-Ossietzky-Universität Oldenburg, Carl-von-Ossietzky-Strasse 9-11, 26111 Oldenburg, Germany

## Results

### Generation of KCNQ4 mouse models

Using homologous recombination in embryonic stem (ES) cells, we created a mouse line with a deletion of *Kcnq4* exons 6–8 and a KI mouse strain carrying the equivalent (G286S) of the human G285S mutation that was identified in a patient with DFNA2 and that exerted strong dominant negative effects (Kubisch *et al*, 1999) (Figure 1A–C and Supplementary Figure S1).

The elimination of exons 6–8 yields a non-functional protein by truncating it at the beginning of the pore-forming P-segment (Figure 1C). The deletion of a carboxy-terminal module that is essential for subunit oligomerization (Schmitt *et al*, 2000; Schwake *et al*, 2003) prevents dominant negative effects on KCNQ3 and KCNQ4 subunits. The dominant negative G286S mutation (Figure 1B), which changes the first glycine of the conserved GYG motif in the P-segment, abolishes channel activity not only in homomeric mutant channels, but also when present in a heteromer with WT subunits (Kubisch *et al*, 1999). This allele is called *Kcnq4*<sup>dn</sup>.

Mice homozygous for either genotype were obtained at approximately Mendelian ratio. Staining for the KCNQ4

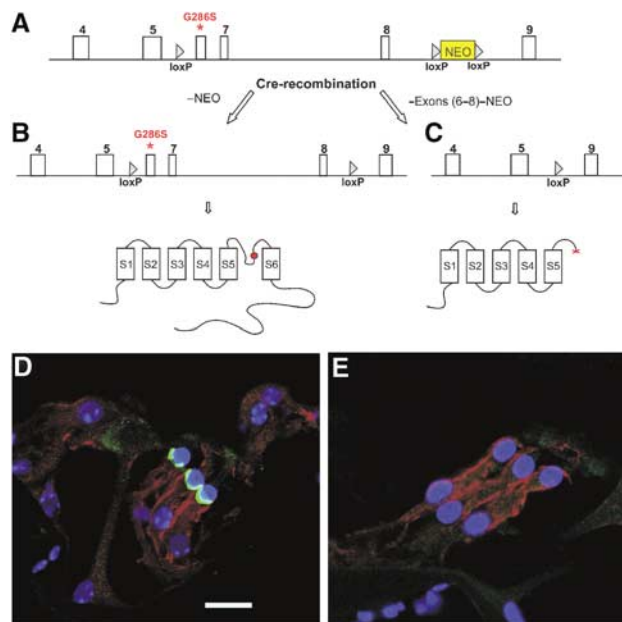


**Figure 1** Generation of KCNQ4-deficient mice. (A) Scheme of mouse genomic *Kcnq4* sequence (exons shown as white boxes) with an insertion of a loxP site in intron 5 and a neomycin selection cassette (NEO) that was flanked by loxP sites in intron 8. A point mutation introduced into exon 6 causes the G286S amino-acid exchange that is equivalent to a mutation found in a patient (Kubisch *et al*, 1999). After homologous recombination in ES cells, treatment with Cre-recombinase yielded two types of clones that were selected for injection into blastocysts: (B) a clone carrying the G286S mutation and two intronic loxP sites (it encodes a channel carrying the dominant mutation in the pore, as indicated by the red ball in the topology model below); (C) a clone in which deletion of exons 6–8 leads to a truncated, non-functional protein schematically shown below. Immunocytochemistry on the organ of Corti of WT (D) and *Kcnq4*<sup>-/-</sup> (E) mice revealed the KCNQ4 protein (green) at the base of WT but not KO OHCs. Supporting Deiters' cells (DC), located at the base of OHCs, are stained for the KCl cotransporter KCC4 (Boettger *et al*, 2002) (red). Nuclei are stained with TOTO (blue). Scale bar: 29 μm (D).

protein revealed its presence at the base of WT OHCs (Figure 1D), as described previously (Kharkovets *et al*, 2000). In contrast, KCNQ4 could not be detected in OHCs from *Kcnq4*<sup>-/-</sup> mice (Figure 1E), a result that also confirmed the specificity of the antibody. Because the expression of the dominant negative allele might be changed by the intronic loxP sites (Figure 1B), mutant mRNA levels were determined by quantitative PCR from brainstem, which also expresses KCNQ4 (Kharkovets *et al*, 2000). Its abundance was indistinguishable from that of the WT message (Supplementary Figure S1C).

Both KCNQ4 mouse models lacked a visible phenotype and displayed normal growth and development. Although KCNQ4 is expressed in type I vestibular hair cells (Kharkovets *et al*, 2000), the vestibular function of KO mice appeared normal. They lacked a circling behaviour and performed equally well in rotarod tests. In histological analysis, the vestibular organ appeared normal (Figure 5H and data not shown). As KCNQ4 is also weakly expressed in the heart (Kubisch *et al*, 1999), electrocardiogram (ECG) analysis was performed. It did not reveal obvious abnormalities (data not shown).

### Evaluation of hearing

We examined auditory function by measuring auditory brainstem responses (ABR) to clicks and tone bursts and otoacoustic emissions. ABR reflect the synchronized electrical activity of the ascending auditory pathway and thus provide information on the sequential processing of acoustical signals in the inner ear and brainstem. Otoacoustic emissions, on the other hand, reflect OHC activity. The nonlinear properties of the cochlear amplifier, which depends on the electromotility of OHCs, leads to emission of multiple frequencies like  $2f_1 - f_2$  when the cochlea is exposed simultaneously to two frequencies  $f_1$  and  $f_2$ . These can be measured as distortion product otoacoustic emissions (DPOAEs) (Robles and Ruggero, 2001).

Auditory brainstem responses to clicks with an upper frequency limit of 5.5 kHz were used to determine hearing thresholds of mice of different genotypes from P14 (14 days after birth) up to the age of 60 weeks (Figure 2A and B). WT animals had a hearing threshold of about 57 dB pe SPL (peak equivalent sound pressure level) that remained stable over time. At P14 (mice begin to hear at P10–11), *Kcnq4*<sup>-/-</sup>, *Kcnq4*<sup>+ / dn</sup> and *Kcnq4*<sup>dn / dn</sup> animals had a higher hearing threshold than controls. However, after an additional week (P21), their hearing ability at these frequencies approached that of WT controls. At that time, ABR latencies and inter-peak intervals of waves I–V were normal (no significant differences (<5%)) (Supplementary Figure S2). As these peaks originate in distinct brainstem regions involved in auditory processing, the loss of KCNQ4 expression in these tracts and nuclei (Kharkovets *et al*, 2000) apparently had no major effect.

Both *Kcnq4*<sup>-/-</sup> and *Kcnq4*<sup>dn / dn</sup> animals thereafter developed a significant hearing loss. In heterozygous dominant negative mice (*Kcnq4*<sup>+ / dn</sup>), the hearing loss was variable and progressed more slowly. Both *Kcnq4*<sup>+ / dn</sup> and *Kcnq4*<sup>dn / dn</sup> animals displayed a threshold shift of about 50–60 dB pe SPL (compared to WT of the same age) at 42 weeks (Figure 2B). In old mice (>12 weeks), the average hearing loss of *Kcnq4*<sup>dn / dn</sup> mice ( $n = 37$ ) was somewhat more pronounced than that of *Kcnq4*<sup>-/-</sup> mice ( $n = 28$ ,  $\Delta \sim 11$  dB;

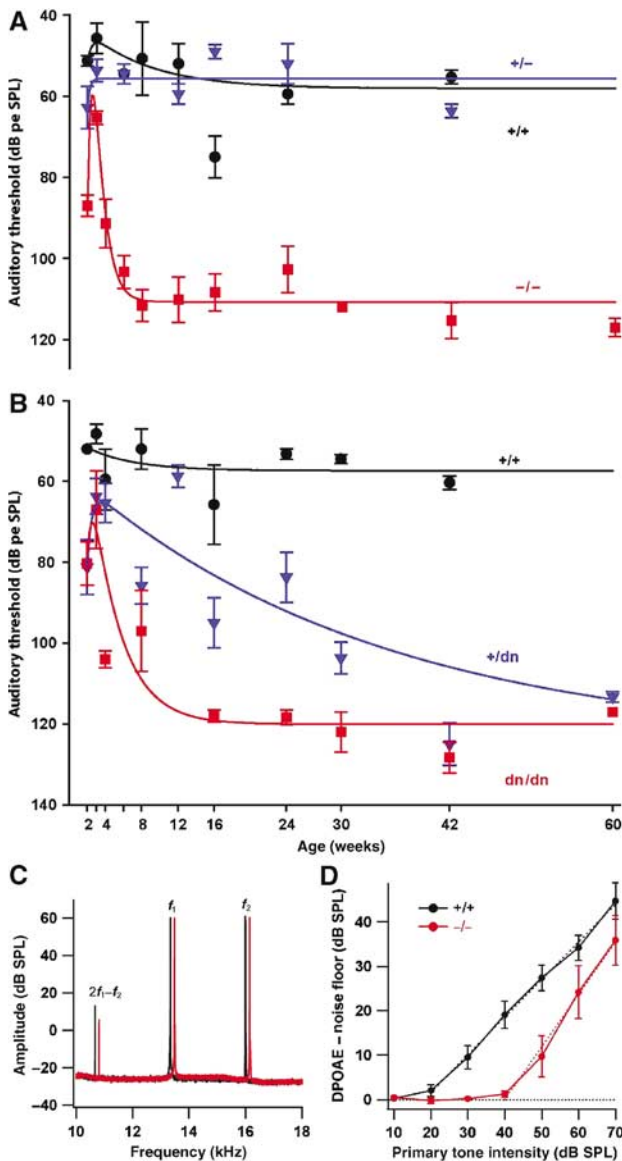


**Figure 2** Hearing ability of *Kcnq4* genotypes as a function of age. (A) Time course of ABR thresholds (low-frequency clicks): *Kcnq4*<sup>+/+</sup> (WT) and *Kcnq4*<sup>+/-</sup> animals have thresholds of ~57 dB pe SPL, which remain constant after the onset of hearing at ~2 weeks. After improving from postnatal day 14 (P14) to ~P21, *Kcnq4*<sup>-/-</sup> (KO) hearing deteriorates rapidly to a constant hearing loss of ~51 dB pe SPL after 8 weeks. (B) ABR thresholds of homo- and heterozygous animals carrying the dominant negative G286S *Kcnq4*<sup>dn</sup> allele compared to WT littermates. In *Kcnq4*<sup>dn/dn</sup> mice, hearing loss progresses as in KO mice to reach ~62 dB pe SPL. *Kcnq4*<sup>+/-dn</sup> mice mimicking heterozygous DFNA2 patients develop deafness much more slowly. (C) Power spectrum of the microphone signal recorded from representative 3-week-old *Kcnq4*<sup>-/-</sup> (red) and *Kcnq4*<sup>+/+</sup> (black) mice showing the 2f<sub>1</sub>-f<sub>2</sub> distortion product otoacoustic emission (DPOAE at 10.7 kHz), as well as the primary tones (f<sub>1</sub> = 13.3 kHz and f<sub>2</sub> = 16 kHz); mutant data are laterally offset for better visibility. (D) Input-output functions for DPOAEs (noise floor subtracted 2f<sub>1</sub>-f<sub>2</sub> DPOAE, f<sub>2</sub> = 16 kHz, six ears for WT (black) and four ears for KO (red)). Dashed lines represent linear approximations of the suprathreshold part of the input-output functions.

$P < 0.001$ ; Figure 2A). No hearing impairment was detected in *Kcnq4*<sup>+/-</sup> animals.

To investigate whether the lack of KCNQ4 affects hair cell function at 3 weeks, when low-frequency clicks revealed only slight, nonsignificant differences in hearing ability and when

OHCs had not yet degenerated (see below), we measured ABR at a higher frequency and determined otoacoustic emissions. In response to a 16 kHz stimulation (that excites the region of high sensitivity in mouse cochlea), the ABR threshold of 3-week-old *Kcnq4*<sup>-/-</sup> mice was shifted by about 35 dB pe SPL compared to controls ( $62.9 \pm 1.8$  dB pe SPL ( $n = 7$ ) for KO versus  $27.8 \pm 2.8$  dB pe SPL ( $n = 9$ ) for WT).

DPOAEs could be recorded from 3-week-old *Kcnq4*<sup>-/-</sup> mice, albeit with lower amplitude (Figure 2C). Consistent with the ABR findings, the average input-output function of DPOAEs showed a shift of about 20 dB (4 KO versus 6 WT mice, f<sub>2</sub> = 16 kHz; Figure 2D). At 8–10 weeks of age, DPOAEs were not distinguishable from the noise floor in *Kcnq4*<sup>-/-</sup> mice, but were readily observed in WT littermates (data not shown).

### Morphological analysis of the inner ear

The morphology of the inner ear was assessed by haematoxylin-eosin (HE) staining of paraffin sections. First, abnormalities were observed in *Kcnq4*<sup>-/-</sup> animals at an age of about 4 weeks, whereas they became detectable in *Kcnq4*<sup>+/-dn</sup> animals only later (Figure 3A–L and Supplementary Table 1). We observed a selective degeneration of OHCs of the basal (high frequency) turn, whereas inner hair cells (IHCs) and the neurons of the spiral ganglion were apparently not affected. The degeneration, which displayed considerable variability between individual animals, progressed over time. Examination of 1-year-old animals revealed a nearly complete loss of OHCs in the basal turn of both *Kcnq4*<sup>-/-</sup> and *Kcnq4*<sup>+/-dn</sup> genotypes (Figure 3J–O and Supplementary Table 1), whereas OHCs of the apical (low frequency) turn were apparently preserved over the entire lifespan. Even at 1 year of age, the degeneration nearly exclusively affected OHCs, while leaving IHCs largely intact. These results were confirmed by staining OHCs with an antibody against the motor protein prestin (Weber *et al*, 2002) and IHCs for calretinin (Dechesne *et al*, 1994) in basal (Figure 3M–O) and apical (Figure 2P–R) turns. A few old (>1 year) *Kcnq4*<sup>-/-</sup> and *Kcnq4*<sup>+/-dn</sup> animals also displayed a loss of IHCs of the basal turn that was associated with a neurodegeneration in the spiral ganglion. However, even in WT animals, some IHC degeneration was occasionally seen in basal turns.

The position of Reissner's membrane, which delimits the scala media, was normal in all genotypes, indicating that salt and fluid secretion by the stria vascularis was not significantly impaired. Although KCNQ4 is expressed in type I vestibular hair cells (Kharkovets *et al*, 2000), histological examination revealed no degeneration in the vestibular organ. We could neither detect morphological changes in the cochlear nucleus, a relay station in the central auditory pathway that expresses KCNQ4 (Kharkovets *et al*, 2000).

The ultrastructure of the organ of Corti was investigated by electron microscopy (Figure 4). At 10 weeks of age, OHCs and IHCs of apical turns were well preserved in the KO (Figure 4B) as compared to WT (Figure 4A). In basal turns, however, OHCs showed cytoplasmic vacuolization that was not observed in the WT (Figure 4C and D). In spite of these degenerative changes in OHCs, the cuticular plate and the tight junctions, which are important for maintaining the electrochemical gradient between the scala media and the perilymph bathing the basolateral membranes of hair cells, appeared intact (Figure 4E and F). High-power electron

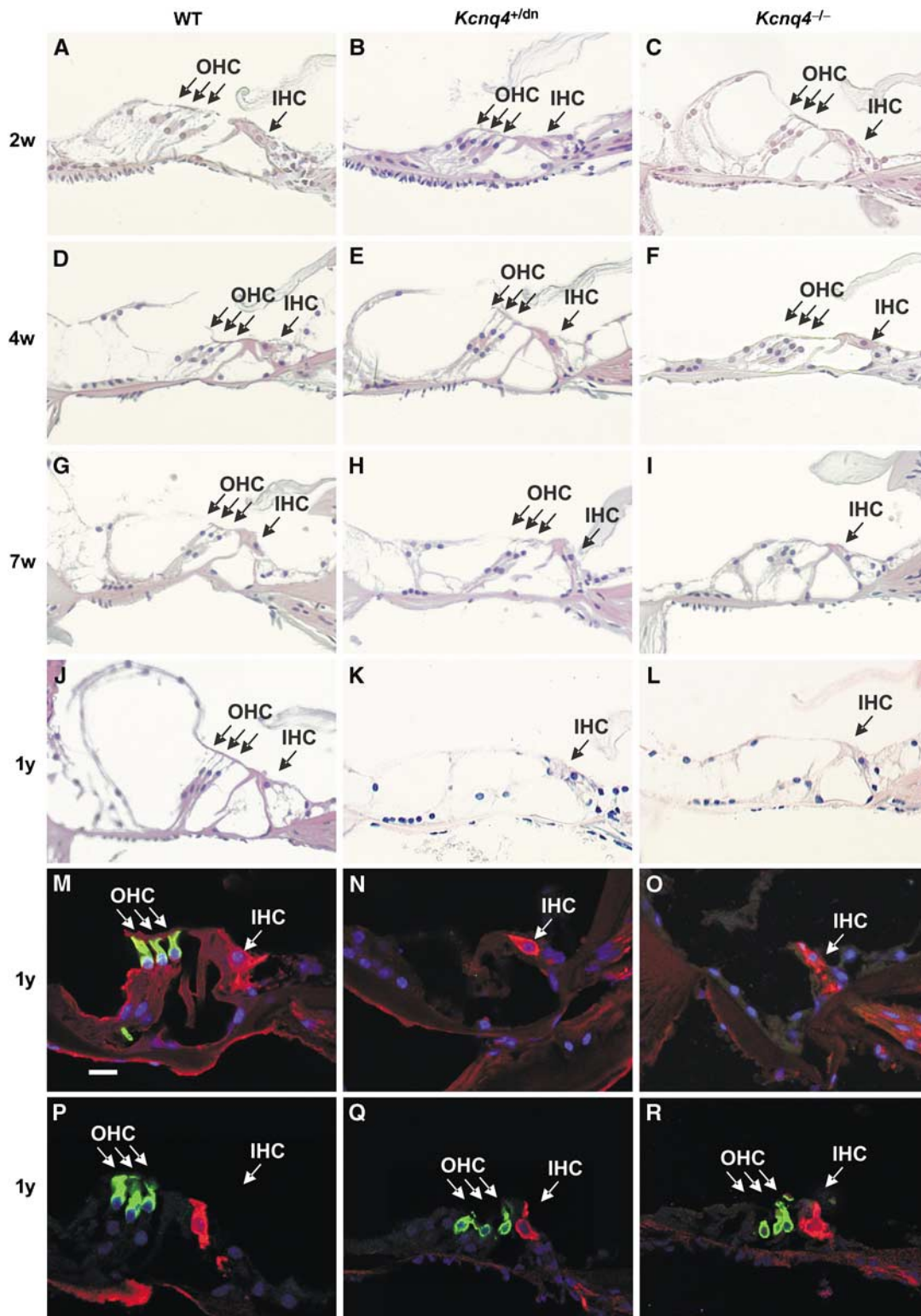


**Figure 3** Degeneration in the organ of Corti. Basal turns of the cochlea of WT, *Kcnq4*<sup>+ /dn</sup> and *Kcnq4*<sup>- /-</sup> (KO) mice (left, centre and right panels, respectively) at ages stated at left were either stained with HE (A–L) or with an antibody against prestin (green) and against calretinin (red) (M–O). As the time course of degeneration varied, representative pictures are shown. No changes were seen in mutated cochleae at P14 (B, C) or P28 (E, F) compared to WT of the same age (A and D, respectively). At 7 weeks (G–I), OHCs of KO mice (I) showed severe degeneration, whereas those of *Kcnq4*<sup>+ /dn</sup> mice (H) remained largely intact. At 1 year of age (J–L), OHCs of both mutants had disappeared, whereas IHCs appeared normal. This was confirmed by staining for the OHC marker prestin and for calretinin, which labels IHCs, in a basal cochlear turn of 1-year-old mice of the three genotypes (P–R). Similar staining of apical turns from 1-year-old mice reveals the presence of both OHCs and IHCs. For a statistical analysis of hair cell degeneration, see Supplementary Table 1. Scale bar: 30  $\mu$ m (M).

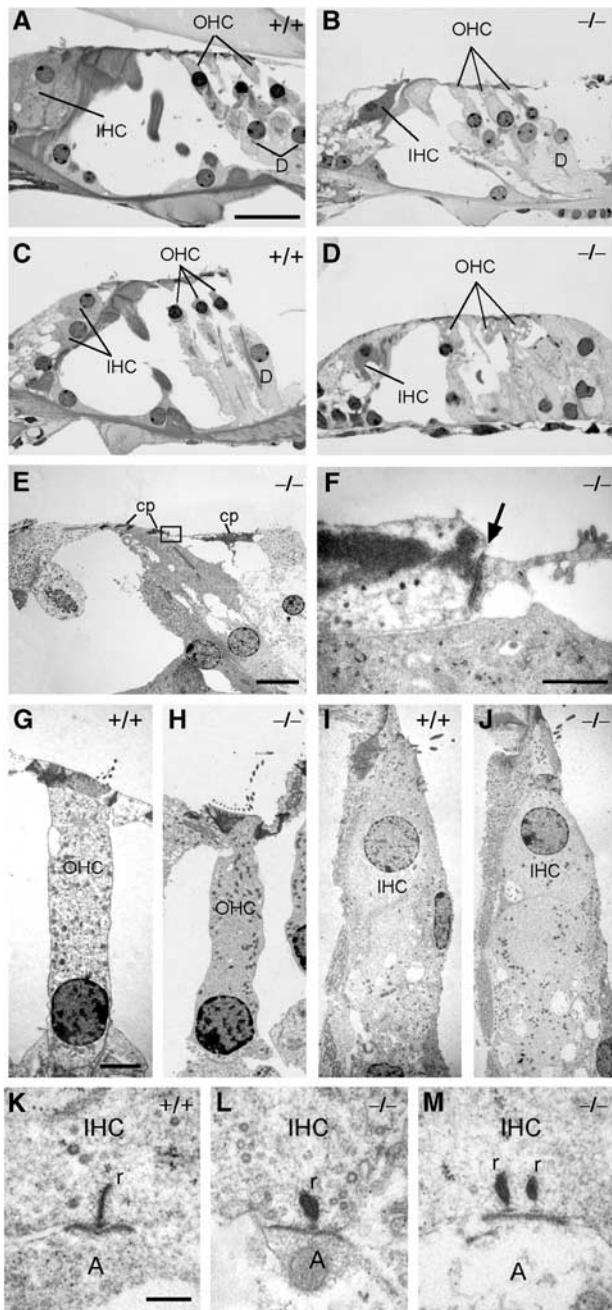


**Figure 4** Semithin sections of apical (A, B) and basal turns (C–E) of 10-week-old WT and *Kcnq4*<sup>-/-</sup> mouse cochleae. Sensory cells in (B) are well preserved, whereas OHCs in (D) show vacuolization of the cytoplasm. Note the presence of the reticular lamina and cuticular plate (cp) in an ultrathin section from a basal turn of a 10-week-old *Kcnq4*<sup>-/-</sup> organ of Corti (E). (F) Higher magnification of the boxed area in (E), with normal tight junction (arrow). (G–J) High-power transmission electron micrographs of 10-week-old (G, H) and 4-month-old (I, J) OHCs and IHCs, respectively, from WT and KO mice in the apical cochlear turn. Even after 4 months, when KO OHCs of basal turns have degenerated, they are morphologically unaltered in the KO. (K–M) Ultrastructural analysis of synaptic zones of IHCs from 4-month-old WT and KO mice. In addition to mature single ribbon synapses (K, L), double ribbon synapses typically found in immature IHCs were found in the KO (M). (r: synaptic ribbon; A: afferent dendrite). Scale bars: 20 μm (A–E), 1 μm (F), 2.5 μm (G–J) and 0.5 μm (K–M).

microscopical pictures of IHCs and OHCs of apical turns of 10-month-old animals did not reveal differences between WT and KO (Figure 4G–J). Except for occasional double ribbon

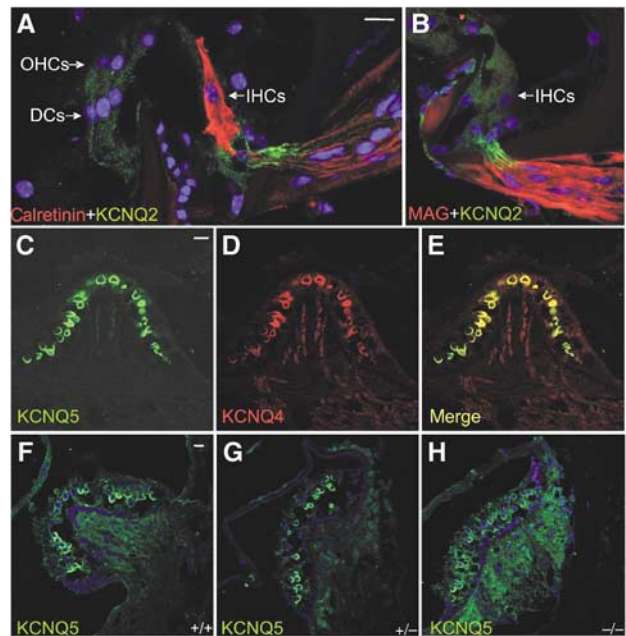


**Figure 5** Expression of KCNQ2 and KCNQ5 in the inner ear. (A) KCNQ2 (green) in afferent fibres of IHCs that are identified by calretinin staining (red). DC: supporting Deiters' cells. (B) Counterstaining for myelin-associated glycoprotein (MAG, red) shows that KCNQ2 (green) is present in unmyelinated segments of the nerve. No KCNQ2 staining is detected in IHCs or OHCs. (C) KCNQ5 is expressed in a subset of vestibular hair cells of the crista ampullaris, which also express KCNQ4 (red) (D) as shown in the overlay (E). (F–H) Vestibular expression of KCNQ5 in WT (F), *Kcnq4*<sup>+/-</sup> (G) and *Kcnq4*<sup>-/-</sup> (H) mice. Scale bars: 29.4 μm.

synapses in the KO (Figure 4M), which are commonly interpreted as a sign of immaturity (Sobkowicz *et al*, 1982), the synaptic zones of KO IHCs did not differ morphologically from WT controls of the same age (4 months) (Figure 4K and L).

As the impact of a loss of KCNQ4 may depend on heteromerization with KCNQ3 or on a coexpression with other KCNQ channels, we investigated their cochlear expression by immunocytochemistry. In the cochlea, KCNQ1 is found exclusively in the apical membranes of marginal cells of the stria vascularis (Neyroud *et al*, 1997). An antibody against KCNQ2 (Cooper *et al*, 2001) failed to label hair cells, but stained apparently unmyelinated segments of axons innervating these cells (Figure 5A and B). An antibody against KCNQ3 (Cooper *et al*, 2001) did not label cochlear structures, although it stained brain sections under the same conditions (Devaux *et al*, 2004) (data not shown). Whereas KCNQ5 was found in vestibular hair cells, where its expression overlapped with KCNQ4 (Figure 5C–E), no specific KCNQ5 signal was detected in the organ of Corti with our own antibody or that of Villarroya and co-workers (Yus-Najera *et al*, 2003).

#### K<sup>+</sup> currents of outer and inner hair cells

Patch-clamp studies of hair cells from the first apical turn were performed on animals from various genotypes at P12–14, that is, before degenerative changes became visible. Resting potentials  $V_R$  of OHCs were measured at zero current in the current clamp mode of the whole-cell configuration with an extracellular solution containing 5.8 mM K<sup>+</sup>. *Kcnq4*<sup>+/+</sup> and *Kcnq4*<sup>+/-</sup> animals showed similar values of

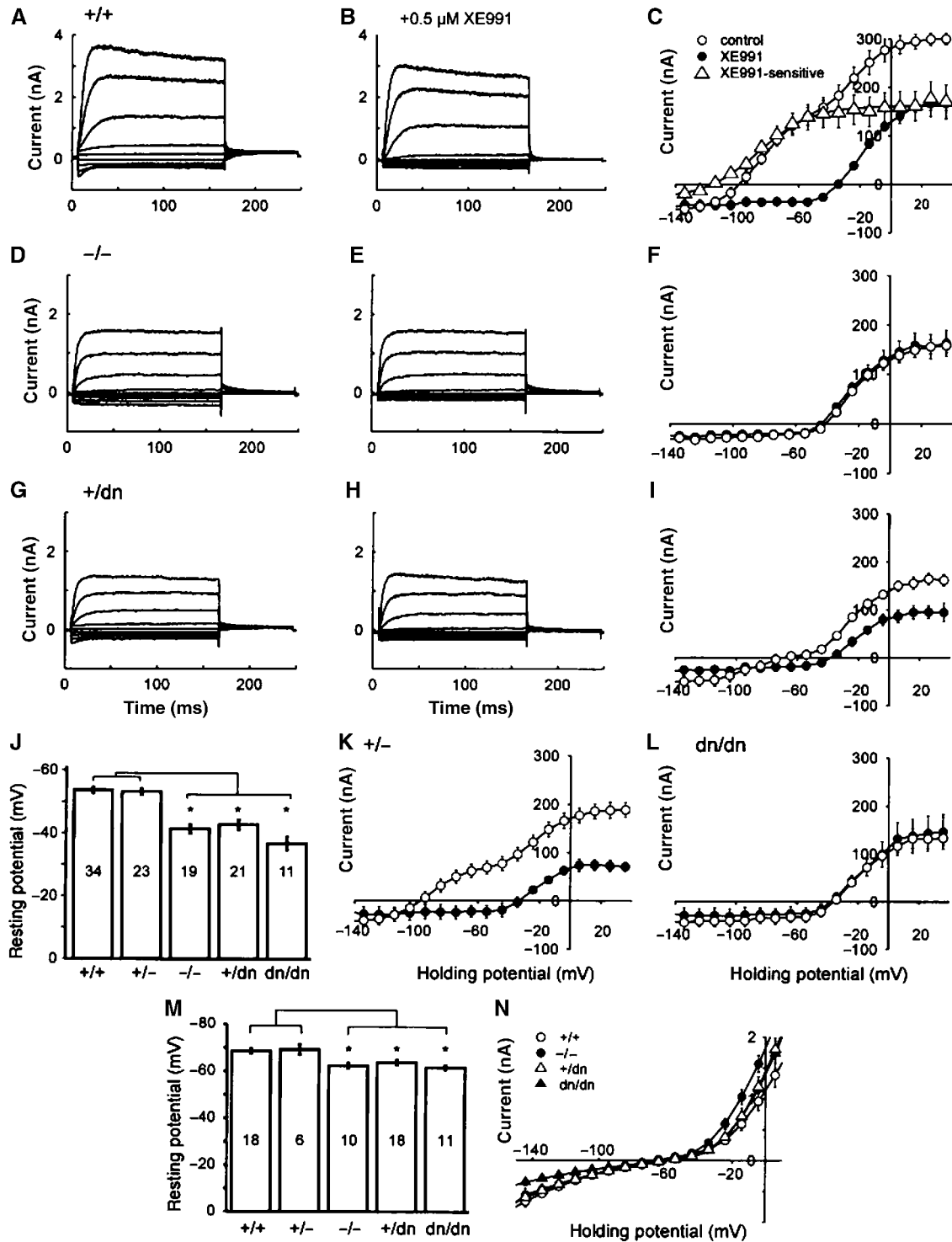


**Figure 6** Patch-clamp analysis of OHCs and IHCs. Representative whole-cell K<sup>+</sup> currents from OHCs of *Kcnq4*<sup>+/+</sup> (A, B), *Kcnq4*<sup>-/-</sup> (D, E) and *Kcnq4*<sup>+dn</sup> (G, H) mice before (A, D, G) and after the application of 0.5 μM XE991 (B, E, H). (C, F, I, K, L) *I/V* curves derived from tail currents in WT (C) and mutated OHCs (F, I, K, L) before (○) and after (●) the application of 0.5 μM XE991. Cells were clamped to voltages between +40 and -140 mV in steps of 10 mV. Values shown are mean ± s.e.m.; *n* = 6–9. There is a significant XE991-sensitive current component in WT (Δ) (C), which was fitted with a Boltzmann function (Supplementary Methods). This component was present neither in KO (*Kcnq4*<sup>-/-</sup>) OHCs (F) nor in *Kcnq4*<sup>dn/dn</sup> mice (L). OHCs of *Kcnq4*<sup>+/-</sup> (K) and *Kcnq4*<sup>+dn</sup> mice (I) have decreased XE991-sensitive currents. (J) Resting membrane potentials of OHCs. OHCs of *Kcnq4*<sup>-/-</sup>, *Kcnq4*<sup>+/-</sup> and *Kcnq4*<sup>dn/dn</sup> mice were depolarized by 10–17 mV compared to WT (*Kcnq4*<sup>+/+</sup>). Asterisks show statistical significance at the *P* ≤ 0.001 level (*t*-test). (M) Resting membrane potentials of IHCs were significantly lower (by 6–8 mV) in *Kcnq4*<sup>-/-</sup>, *Kcnq4*<sup>dn/dn</sup> and *Kcnq4*<sup>+dn</sup> mice than in WT and *Kcnq4*<sup>+/-</sup> animals (*P* ≤ 0.005, *t*-test). In (J, M), numbers in bars indicate the number of measurements *n*, error bars s.e.m. (N) *I/V* relationship of the hyperpolarizing whole-cell K<sup>+</sup> currents of IHCs (Supplementary Figure S3). Differences between *Kcnq4*<sup>+/+</sup> and *Kcnq4*<sup>+dn</sup> mice are significant at -150 mV. Values are given as the mean ± s.e.m.; *n* = 5–11. In *I/V* curves, data points were connected by lines, except for the Boltzmann fit of XE991-sensitive currents in (C).

$V_R = -58.0 \pm 0.9$  and  $-57.4 \pm 1$  mV, respectively. By contrast, OHCs from *Kcnq4*<sup>-/-</sup>, *Kcnq4*<sup>+ /dn</sup> and *Kcnq4*<sup>dn/dn</sup> mice were depolarized by about 10–17 mV compared to WT ( $V_R = -45.6 \pm 1.4$ ,  $-46.9 \pm 1.6$  and  $-41.0 \pm 2.1$  mV, respectively) (Figure 6J).

In WT OHCs, depolarizing pulses induced slowly activating and partially inactivating outward currents. At 40 mV, steady-state current amplitude reached  $93 \pm 3\%$  of the peak current amplitude ( $n = 13$ , *Kcnq4*<sup>+/+</sup> OHC; Figure 6A). Activation time constants of these currents were derived from monoexponential fits to the first 16 ms after stimulus onset and ranged from  $20 \pm 3$  ms at  $-20$  mV to  $6 \pm 1$  ms at 40 mV. Hyperpolarizing steps led to instantaneous inward currents (Figure 6A) that deactivated with an approximately monoexponential time course. Time constants ranged from  $10 \pm 1$  ms at  $-140$  mV to  $23 \pm 3$  ms at  $-110$  mV ( $n = 13$ , *Kcnq4*<sup>+/+</sup> OHC). XE991 (0.5  $\mu$ M), a selective inhibitor of KCNQ channels (Wang *et al*, 1998), inhibited the instantaneous inward current components in response to hyperpolarizing voltage steps and decreased the amplitude of the outward currents (Marcotti and Kros, 1999) (Figure 6A–C). *I/V* curves obtained from tail current analysis (Figure 6C) showed that, in the WT, K<sup>+</sup> currents activated already at voltages more negative than  $-100$  mV. Inhibition by XE991 revealed that a major component of the KCNQ-independent current component activated at a threshold of about  $-40$  mV. The XE991-sensitive current component activated at roughly  $-120$  mV. Fitting the current–voltage relationship with a Boltzmann function yielded a half-maximal activation of  $V_{1/2} = -86 \pm 1.6$  mV for the XE991-sensitive component (Figure 6C). This component was significantly reduced in *Kcnq4*<sup>+/-</sup> mice (Figure 6K). In *Kcnq4*<sup>-/-</sup> (Figure 6D–F) and *Kcnq4*<sup>dn/dn</sup> mice (Figure 6L), it was completely abolished. A small portion of these currents was still measured in *Kcnq4*<sup>+ /dn</sup> animals (Figure 6G–I). XE991 application did not influence the resting membrane potential in *Kcnq4*<sup>-/-</sup> and *Kcnq4*<sup>dn/dn</sup> mice, whereas it depolarized WT OHCs. Effects of the drug were poorly reversible; therefore, the preparation was discarded after XE991 application.

Compared to OHCs, resting membrane potentials of WT IHCs were more hyperpolarized ( $V_R = -68.6 \pm 1.1$  mV) (Figure 6M). The disruption of *Kcnq4* led to a depolarization of IHCs. In line with our inability to detect KCNQ4 in IHCs by immunocytochemistry (Kharkovets *et al*, 2000), this depolarization (by 6–8 mV) was much less pronounced than in OHCs ( $V_R = -62.4 \pm 1.1$  mV for *Kcnq4*<sup>-/-</sup>,  $V_R = -63.8 \pm 1.1$  mV for *Kcnq4*<sup>+ /dn</sup> and  $V_R = -61.6 \pm 1$  mV for *Kcnq4*<sup>dn/dn</sup>). Differences within the groups of mice carrying different KCNQ4 mutations were again not significant. We were unable to detect a clear XE991-sensitive current component in WT IHCs, although the inhibitor depolarized these cells by 3–5 mV. Membrane currents of IHC differed in the transient response to hyperpolarization (Supplementary Figure S3). We, therefore, analysed the voltage dependence of activation 11 ms after the onset of the voltage change. IHC of *Kcnq4*<sup>-/-</sup> and *Kcnq4*<sup>dn/dn</sup> mice showed smaller inward currents than *Kcnq4*<sup>+/+</sup> and *Kcnq4*<sup>+ /dn</sup> mice (Figure 6N and Supplementary Figure S3).

#### Presynaptic function of inner hair cells

Ca<sup>2+</sup> currents and exocytosis in apical IHCs of mature *Kcnq4*<sup>-/-</sup> mice were studied at 8 weeks, when hearing was

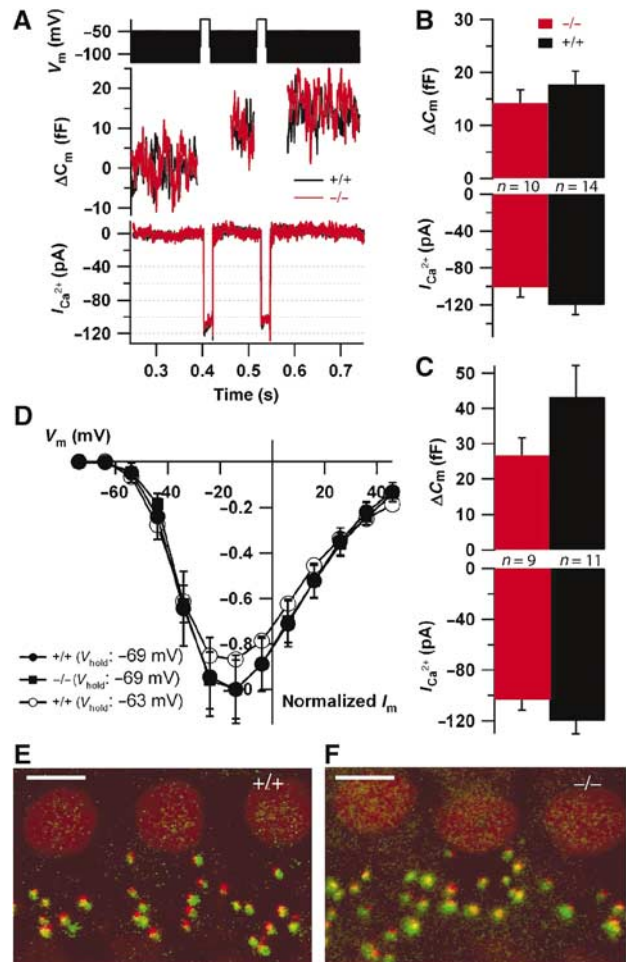


**Figure 7** Presynaptic properties of IHCs. (A)  $\Delta C_m$  responses (middle) and Ca<sup>2+</sup> currents (bottom) of two representative *Kcnq4*<sup>-/-</sup> and WT IHCs to a  $2 \times 20$  ms depolarization to  $-24$  mV (top; black bar represents the 70 mV peak-to-peak, 1 kHz sine wave potential used for  $C_m$  estimation). The 40 ms of the  $C_m$  following stimulation were disregarded because of a conductance-related artefact (same in B, D). (B) Average  $\Delta C_m$  (top) and Ca<sup>2+</sup> currents (bottom) evoked by  $2 \times 20$  ms depolarization in *Kcnq4*<sup>-/-</sup> ( $n = 10$ ) and WT ( $n = 14$ ) IHCs. (C) Responses to  $2 \times 50$  ms double-pulse depolarizations ( $n = 9$  for KO and  $n = 11$  for WT). The differences between genotypes in (B, C) are not statistically significant. (D) Ca<sup>2+</sup> current *I/V* relationships of WT IHCs (●) and KO IHCs (○) when holding at the resting potential of WT IHCs ( $-69$  mV, normalized to their respective peak currents), and of WT IHCs when holding at the resting potential of KO IHCs ( $-63$  mV (○), normalized to the mean WT peak current elicited from a holding potential of  $-69$  mV). (E, F) Representative montages of confocal stacks obtained from WT (E) and KO (F) organs of Corti immunostained for the presynaptic ribbon (green, Ribeye/CtBP2; Schmitz *et al*, 2000) and postsynaptic glutamate receptors (red, GluR2/3). In both whole mounts, ribbons and dendrites are mostly juxtaposed, indicating intact gross synapse morphology with anchored ribbons. Scale bars: 5  $\mu$ m.

already severely reduced (Figure 2A). For comparing the intrinsic presynaptic function, cells were stimulated from a hyperpolarized potential ( $-74$  mV). Figure 7A displays representative Ca<sup>2+</sup> currents and exocytotic capacitance changes of WT and *Kcnq4*<sup>-/-</sup> IHCs in response to 20 ms double-pulse depolarizations to test for fast exocytosis (Moser and Beutner, 2000). These were not significantly different between genotypes (Figure 7B). Similar findings were obtained with 50 ms double-pulse depolarizations (Figure 7C), which mainly test

the slow component of exocytosis (Moser and Beutner, 2000). The voltage dependence of Ca<sup>2+</sup> current activation from a holding potential of -69 mV (resting potential of WT IHCs; Figure 6M) was unchanged in *Kcnq4*<sup>-/-</sup> IHCs (Figure 7D). To mimic the effect of the slight depolarization of KO IHCs, Ca<sup>2+</sup> currents were measured after a 20 s long pre-depolarization to the potential of *Kcnq4*<sup>-/-</sup> IHCs (-62.4 mV; Figure 6M). The small and nonsignificant reduction of the peak Ca<sup>2+</sup> current (Figure 7D) is unlikely to cause a major block of IHC exocytosis.

Immunostaining of afferent IHC synapses (Figure 7E and F) for presynaptic ribbons (Ribeye, green) (Khimich *et al*, 2005) and postsynaptic glutamate receptors (GluR2/3, red) revealed comparable numbers of ribbon-containing afferent synapses (11.9 ± 0.7 for KO, *n* = 60 IHCs of four ears and 12.1 ± 0.5 for WT, *n* = 42 IHCs of four ears). Consistent with the electron microscopy (Figure 4K and L), these data suggest that synapse morphology in the KO is intact.

## Discussion

In order to understand the mechanisms underlying the slowly progressive hearing loss in autosomal dominant DFNA2, we have generated and analysed two different KCNQ4 mouse models. Mice heterozygous for a KI of a dominant negative mutation found in patients (Kubisch *et al*, 1999) closely reflect the pathology of DFNA2. The second model, a complete KO of the KCNQ4 potassium channel, provides a loss-of-function model for KCNQ4 and hence a better understanding of the physiological roles of KCNQ4.

Our mouse models recapitulate the slowly progressive hearing loss in DFNA2 patients. Fortunate from an experimental point of view, the rate of progression is much faster in these mice than in humans, in whom the hearing loss develops over decades (Coucke *et al*, 1999; De Leenheer *et al*, 2002). The total KO of KCNQ4 caused a more rapid progression towards deafness than the heterozygous presence of the dominant negative mutant. This suggests that the presence of 1/16 of KCNQ4 currents, which is predicted to remain with tetrameric K<sup>+</sup> channels upon heterozygous expression of a strong dominant mutant, may lead to a significant delay in hair cell degeneration. Mice heterozygous for the total KO showed no hearing abnormalities, implying that 50% of currents are sufficient for normal function.

KCNQ4 not only forms functional homo-oligomers, but can also assemble with KCNQ3 to form hetero-oligomeric channels (Kubisch *et al*, 1999) that will also be functionally suppressed by the dominant negative KCNQ4 mutation. RT-PCR on RNA from whole cochleae had revealed the presence of KCNQ3 message (Kubisch *et al*, 1999). However, we were unable to detect KCNQ3 in cochlear sections by immunofluorescence with a KCNQ3 antibody that works in immunohistochemistry on brain tissue (Devaux *et al*, 2004). This discrepancy might be explained by the higher sensitivity of the PCR technique. The apparently complete loss of XE991-sensitive currents in the total KO (Figure 5D) argues against a significant presence of KCNQ3 in OHCs. However, as homomeric KCNQ3 yields only small currents (Schroeder *et al*, 1998; Kubisch *et al*, 1999), we cannot rule out that OHCs express low levels of KCNQ3. The observation that *Kcnq4*<sup>dn/dn</sup> mice display a slightly more pronounced hearing loss than

KO mice (Figure 2) might then be interpreted as a dominant negative effect on KCNQ3.

The present mouse models support our previous hypothesis that the slow progression of DFNA2 hearing loss is due to a chronic depolarization and subsequent degeneration of OHCs that ensues from the loss of a major OHC K<sup>+</sup> efflux pathway (Kubisch *et al*, 1999; Kharkovets *et al*, 2000). In WT animals, the *I*<sub>K,n</sub> current is already present to some degree at the normal resting potential. Owing to the lack of this current, KO OHCs were depolarized by about 10–17 mV. This depolarization may increase Ca<sup>2+</sup> influx through voltage-gated Ca<sup>2+</sup> channels, which may constitute a chronic stress for the cells and lead to their degeneration. Depolarizing OHCs by raising extracellular K<sup>+</sup> was previously shown to have deleterious short- and long-term effects on OHCs (Zenner *et al*, 1994). Interestingly, the KO of the  $\alpha$ -subunit of the BK channel, a Ca<sup>2+</sup>-activated K<sup>+</sup> channel that is also expressed in hair cells, led to deafness in mice as well (Rüttiger *et al*, 2004).

At first, our mice, just as DFNA2 patients, showed only a slight hearing impairment. At that time, we found reduced DPOAEs despite normal counts of OHCs. Several mechanisms might contribute to the reduced cochlear amplification. Firstly, the observed OHC depolarization of 10–17 mV would decrease the mechano-electrical transduction current by lowering the driving force for apical K<sup>+</sup> influx that normally amounts to about 150–160 mV. This would reduce both stereociliar (Chan and Hudspeth, 2005; Kennedy *et al*, 2005) and somatic (Zheng *et al*, 2000; Liberman *et al*, 2002) amplification mechanisms. Secondly, the lack of KCNQ4 reduced the membrane conductance at physiological voltages. The resulting increase of the membrane time constant would cause a major reduction of the AC component of the receptor potential, resulting in a decreased somatic (prestin-mediated) amplification. Thirdly, the depolarization may reduce the dynamic range of the somatic OHC amplification by shifting its operating point away from the optimal voltage.

In contrast to OHCs, a degeneration of IHCs was observed only in rare cases in old animals. It was limited to basal turns of the cochlea. The morphology and *in vitro* function of afferent IHC synapses appeared normal as well (Figures 4K–M and 7). Satisfyingly, the extent of the mean maximum hearing loss in our mice (50–60 dB) is compatible with a selective loss of OHCs, electromotile cells that amplify the mechanical vibration. The selective pharmacological ablation of OHCs led to a hearing loss of about 30–50 dB (Ryan and Dallos, 1975) and the genetic ablation of the motor protein prestin increased the hearing threshold by 40–60 dB (Liberman *et al*, 2002). Accordingly, the 16 kHz DPOAEs, which reflect the amplifying properties of high-frequency OHCs, were absent in 3-month-old KO animals. The preferential degeneration of OHCs in basal, high-frequency turns correlates with the clinical observation that DFNA2 hearing loss preferentially affects high frequencies (De Leenheer *et al*, 2002).

In patients with DFNA2, the hearing loss is not complete either. It typically reaches 40–60 dB at 1 kHz at about 50 years of age (De Leenheer *et al*, 2002). At later ages, however, hearing loss can exceed 80 dB at 1 kHz and can even be more severe at higher frequencies. Because such an extent of hearing loss cannot be explained by a loss of OHCs alone, there might be an additional impairment of IHCs at an age when presbycusis sets in.

The slight depolarization of IHCs agrees with the detection of KCNQ4 mRNA (Beisel *et al*, 2000; Kharkovets *et al*, 2000) and  $I_{K,n}$ -like currents in IHCs (Marcotti *et al*, 2003; Oliver *et al*, 2003). Oliver *et al* (2003) have suggested that a loss of KCNQ4 may cause DFNA2 deafness via a degeneration of IHCs caused by an increase of their  $[Ca^{2+}]_i$ . The present data, however, argue against IHC dysfunction or degeneration as a major mechanism in DFNA2. The depolarization could potentially impair afferent synaptic transmission by inactivation of IHC  $Ca^{2+}$  channels. We failed to detect any obvious functional or morphological synaptic defects (Figure 7). Moreover, we did not observe significant changes in pre-synaptic  $Ca^{2+}$  currents upon chronic depolarization to the putative resting potential of *Kcnq4*<sup>-/-</sup> IHCs. Therefore, it is unlikely that an IHC synaptic defect contributes largely to DFNA2 pathology. Our work neither supports the hypothesis that a differential expression of KCNQ4 in IHCs and sensory neurons is the basis of DFNA2 (Beisel *et al*, 2005).

Although KCNQ4 is highly expressed in type I vestibular hair cells (Kharkovets *et al*, 2000), neither the total KO nor the dominant negative line showed vestibular symptoms. Also patients with DFNA2 do not display vestibular symptoms. We have shown here that the vestibular cells that express KCNQ4 also express KCNQ5 (Figure 5C–E), suggesting that KCNQ5 may compensate the loss of KCNQ4, although it is not upregulated in the KO (Figure 5F–H). Future patch-clamp experiments may clarify this issue and could reveal whether KCNQ4 mediates the  $g_{K,1}$  current of vestibular hair cells (Correia and Lang, 1990), as postulated previously (Kharkovets *et al*, 2000).

An important conclusion from the present study is that the  $I_{K,n}$  current in OHCs (Housley and Ashmore, 1992) is mediated by KCNQ4. Such a role of KCNQ4 had been proposed on the basis of a biophysical and pharmacological comparison between  $I_{K,n}$  and KCNQ4 currents (Marcotti and Kros, 1999; Kharkovets *et al*, 2000) and by the localization of KCNQ4 and  $I_{K,n}$  currents to the basal pole of OHCs (Nakagawa *et al*, 1994; Santos-Sacchi *et al*, 1997; Kharkovets *et al*, 2000). However, in heterologous expression in oocytes, KCNQ4 activates at voltages that are 70–80 mV more positive than  $I_{K,n}$  (Housley and Ashmore, 1992; Mammano and Ashmore, 1996; Kubisch *et al*, 1999; Marcotti and Kros, 1999). In transfected mammalian cells (Sogaard *et al*, 2001; Chambard and Ashmore, 2005), KCNQ4 activates at voltages that are ~20 mV more negative than observed in oocytes. The absence of  $I_{K,n}$  currents in *Kcnq4*<sup>-/-</sup> OHCs now demonstrates that these are mediated by KCNQ4, either in a homomeric or heteromeric complex. Several possibilities to explain the differences in voltage dependence come to mind: OHCs may express KCNQ4-interacting proteins that are lacking in heterologous expression, or KCNQ4 gating may be influenced by post-translational modifications or interactions with small intracellular molecules. Recently, it was suggested that KCNQ4 phosphorylation via PKA and coupling to a complex that may include prestin leads to the negative shift of the voltage for activation of KCNQ4 (Chambard and Ashmore, 2005).

In a recent pharmacological study, linopirdine, an inhibitor of several KCNQ isoforms (KCNQ2–5), was infused at concentrations of up to 1 mM into cochleae of guinea-pigs, either acutely or up to 7 days (Nouvian *et al*, 2003). Although the resulting reduction of otoacoustic emissions and the selective

degeneration of OHCs agree with the present study, the irreversibility of drug effects even after short application and the very fast degeneration of OHCs (Nouvian *et al*, 2003) argue for additional toxic effects on OHCs. Furthermore, linopirdine may have additional effects by inhibiting KCNQ2 on cochlear neurons that innervate hair cells (Figure 5A and B), or by blocking nicotinic acetylcholine receptors of OHCs and IHCs (Gómez-Casati *et al*, 2004).

In summary, our mouse models faithfully reproduce human deafness of DFNA2 type and have revealed that slowly developing hearing loss is mainly caused by a degeneration of OHCs. In addition, the loss of the KCNQ4-dependent  $I_{K,n}$  current affects OHC amplification, most likely as a consequence of OHC depolarization. The dominant negative KI strain, which directly replicates a human DFNA2 mutation, provides a valuable model system for DFNA2 and for slowly developing deafness in general. Indeed, hearing loss in the elderly is the most common sensory defect in humans with a huge impact on the individuals and society. The present mouse model may be useful to test pharmacological strategies (e.g. K<sup>+</sup> channel openers) to delay the progression of deafness.

## Materials and methods

### Generation of mice with an altered KCNQ4 gene

Genomic sequence was obtained from a mouse ES cell line (MPI-2, derived from a 129SvJ mouse strain). A fragment of genomic DNA was amplified using primers in introns 1 and 10 and was cloned in the pKO-V901 vector (Lexicon Genetics). A loxP site was inserted by PCR between exons 5 and 6, and a 'floxed' neomycin resistance (NEO) cassette between exons 8 and 9 by ligation into an *Eco47III* site (Figure 1). A diphtheria toxin A cassette was fused 5'. For the KI, the mutation G286S (equivalent to human G285S) was additionally inserted into exon 6. Sequenced constructs were electroporated into MPI2 ES cells. Clones having undergone homologous recombination were transfected with a plasmid expressing Cre-recombinase. Cells with an exclusive deletion of the NEO cassette were used to generate mice with 'floxed' and dominant negative alleles, and those with deleted exons 6–8 (leading to a frameshift) for the KO line. Cells were injected into C57BL/6 blastocysts that were implanted into foster mothers. The resulting chimeras were bred with C57BL/6 females. Heterozygous animals stemming from two different ES cell clones were inbred to yield mutant mice. Experiments were performed on littermates with C57BL/6-129SV mixed background. For primer sequences, see Supplementary data.

### Evaluation of hearing

Animals were anaesthetized with Ketamin/Rompun and kept warm. Electrodes were placed subcutaneously on the head (reference electrode at the vertex and active electrodes at both mastoids). The ABR stimuli consisted of 200  $\mu$ s (low frequency) clicks with a flat spectrum up to 5.5 or 16 kHz tone bursts. Averaged responses were amplified with band-pass setting of 50–2500 Hz. Near the threshold, the intensity was varied in steps of 5 dB and responses for 2000 sweeps were averaged at each intensity level. The hearing threshold was defined as the lowest intensity to generate a reproducible ABR waveform.

For DPOAE, a 24-bit sound card together with the ED1/EC1 speaker system (Tucker-Davis) was used to generate two primary tones ( $f_1$  and  $f_2$ ) with a ratio of  $f_2/f_1 = 1.2$  and  $f_2 = 16$  kHz. Primary tones were coupled into the ear canal by a custom-made probe containing an MKE-2 microphone (Sennheiser) and adjusted to an intensity of 60 dB sound pressure level at the eardrum. The microphone signal was amplified (DMP3, MIDIMAN) and analysed by fast Fourier transformation.

### Histological analysis and immunocytochemistry

Inner ears were dissected from the temporal bone and fixed at 4°C for 1.5 h in 4% PFA in PBS. From P8 onwards, bones were decalcified with rapid decalcifier and postfixed with 4% PFA for 15 min. For immunohistological staining, 8 µm cryosections were prepared after incubation in 30% sucrose in PBS and embedding in Tissue Freezing Medium (Leica). Sections were blocked with 3% normal goat serum (NGS), 2% BSA and 0.5% NP-40 in PBS. Primary and secondary fluorescence-labelled antibodies were applied in PBS with 3% normal goat serum and 0.1% NP-40. For investigating IHC ribbon synapses, whole-mount immunohistochemistry was used. The following primary antibodies were used: rabbit anti-KCNQ4 (K4C; Kharkovets *et al*, 2000), anti-prestin (Weber *et al*, 2002), anti-calretinin (Swant), anti-CtBP-2 mouse monoclonal (Becton-Dickinson), rabbit anti-GluR2/3 (Chemicon) and anti-KCNQ2 rabbit polyclonal (Cooper *et al*, 2001). A rabbit antiserum was generated against the peptide KLSLVQNLIRSTEELN-amide that represents KCNQ5 residues 793–808. The affinity-purified serum was specific as shown by Western blotting and immunocytochemistry of KCNQ5-transfected HEK cells. Secondary antibodies were Alexa Fluor 568 goat anti-mouse IgG and Alexa Fluor 488 goat anti-rabbit IgG (Molecular Probes). TOTO<sup>®</sup>-3 iodide was used for staining nuclei. For HE staining, tissue specimens were paraffin-embedded and sectioned to 5 µm.

### Preparation of semithin and ultrathin sections

Cochleae from three anaesthetized KO and WT animals (age: 10 weeks and 4 months) were quickly removed and perfused through the round window with 3% glutaraldehyde in PBS and left in the fixative overnight, decalcified for 3 days in 10% EDTA (pH 7.3) at 4°C, cut in two, postfixed in 2% osmium tetroxide for 30 min, dehydrated in a graded series of ethanol solutions and embedded in Epon. The blocks were cut in semithin (0.5 µm) and ultrathin (60 nm) sections. Semithin sections were stained with methylene blue. Ultrathin sections stained with uranyl acetate and lead citrate were examined with a Zeiss 902 electron microscope.

### Patch-clamp measurements of hair cells

Cochleae were dissected and kept in cold preparation solution, which contained (in mM) 144 NaCl, 5.8 KCl, 0.1 CaCl<sub>2</sub>, 2.1 MgCl<sub>2</sub>, 0.7 NaH<sub>2</sub>PO<sub>4</sub>, 5.6 glucose and 10 HEPES. The apical turn of the cochlea was dissected, fixed with a nylon net on the coverslip and perfused with the bath solution (in mM: 144 NaCl, 5.8 KCl, 2 CaCl<sub>2</sub>,

0.9 MgCl<sub>2</sub>, 0.7 NaH<sub>2</sub>PO<sub>4</sub>, 5.6 glucose, 10 HEPES, pH 7.3). Patch-clamp measurements employed the whole-cell configuration. After equilibrating the cell interior with the pipette solution (in mM: 135 KCl, 3.5 MgCl<sub>2</sub>, 0.1 CaCl<sub>2</sub>, 2.5 Na<sub>2</sub>-ATP, 5 EGTA, 5 HEPES, pH 7.3), the resting potential was measured as the zero-current voltage in the current clamp mode of the patch-clamp amplifier. For the clamp protocol and additional details, see Supplementary Methods.

### Ca<sup>2+</sup> currents and capacitance measurements of inner hair cells

For recording Ca<sup>2+</sup> currents and ΔC<sub>m</sub>, the pipette contained (in mM) 130 Cs-gluconate, 10 TEA-Cl, 10 4-AP, 10 CsOH-HEPES, 1 MgCl<sub>2</sub> and amphotericin B (Calbiochem; up to 250 µg/ml) and the extracellular solution (105 NaCl, 35 TEA-Cl, 2.8 KCl, 2 CaCl<sub>2</sub>, 1 MgCl<sub>2</sub>, 10 NaOH-HEPES, 10 glucose). Currents were sampled at 20 kHz and low-pass filtered at 2 kHz using EPC-9 amplifiers controlled by 'Pulse'-software (HEKA). C<sub>m</sub> was measured using the Lindau-Neher technique (Lindau and Neher, 1988). Currents were leak-corrected and only cells with a leak current < -40 pA at -74 mV and an access resistance of < 30 MΩ were analysed further. Voltages were corrected for liquid junction potentials (14 mV). ΔC<sub>m</sub> was estimated as the difference of the mean C<sub>m</sub> after the end of the depolarization and the mean pre-pulse C<sub>m</sub> (the initial 100 ms after the depolarization were skipped) and averaged for each stimulus in a given cell. The grand averages of Ca<sup>2+</sup> current amplitudes and ΔC<sub>m</sub> for a stimulus were calculated from mean estimates of individual cells contributing more than three responses to 20 ms, were expressed ± s.e.m. and compared for statistical differences using the unpaired *t*-test.

### Supplementary data

Supplementary data are available at *The EMBO Journal Online*.

### Acknowledgements

We thank D Oliver and B Fakler for advising K Dedek on patch-clamping cochlear hair cells, A Zdebek for ECG measurements, M Knipper for the prestin antibody, T Boettger for advice on cochlear immunohistochemistry, A Villarreal for his KCNQ5 antibody and E Cooper for antibodies against KCNQ2 and KCNQ3. This work was supported by grants from the European Union (FP5 and FP6) to TJJ and a grant of the DFG (CMPB) to TM.

### References

- Beisel KW, Nelson NC, Delimont DC, Fritsch B (2000) Longitudinal gradients of KCNQ4 expression in spiral ganglion and cochlear hair cells correlate with progressive hearing loss in DFNA2. *Brain Res Mol Brain Res* **82**: 137–149
- Beisel KW, Rocha-Sanchez SM, Morris KA, Nie L, Feng F, Kachar B, Yamoah EN, Fritsch B (2005) Differential expression of KCNQ4 in inner hair cells and sensory neurons is the basis of progressive high-frequency hearing loss. *J Neurosci* **25**: 9285–9293
- Boettger T, Hübner CA, Maier H, Rust MB, Beck FX, Jentsch TJ (2002) Deafness and renal tubular acidosis in mice lacking the K-Cl co-transporter *Kcc4*. *Nature* **416**: 874–878
- Boettger T, Rust MB, Maier H, Seidenbecher T, Schweizer M, Keating DJ, Faulhaber J, Ehmke H, Pfeffer C, Scheel O, Lemcke B, Horst J, Leuwer R, Pape HC, Völkl H, Hübner CA, Jentsch TJ (2003) Loss of K-Cl co-transporter *KCC3* causes deafness, neurodegeneration and reduced seizure threshold. *EMBO J* **22**: 5422–5434
- Chambard JM, Ashmore JF (2005) Regulation of the voltage-gated potassium channel KCNQ4 in the auditory pathway. *Pflügers Arch* **450**: 34–44
- Chan DK, Hudspeth AJ (2005) Ca<sup>2+</sup> current-driven nonlinear amplification by the mammalian cochlea *in vitro*. *Nat Neurosci* **8**: 149–155
- Cooper EC, Harrington E, Jan YN, Jan LY (2001) M channel KCNQ2 subunits are localized to key sites for control of neuronal network oscillations and synchronization in mouse brain. *J Neurosci* **21**: 9529–9540
- Corey DP, García-Añoveros J, Holt JR, Kwan KY, Lin SY, Vollrath MA, Amalfitano A, Cheung ELN, Derfler BH, Duggan A, Géléoc GS, Gray PA, Hoffman MP, Rehm HL, Tamasauskas D, Zhang DS (2004) TRPA1 is a candidate for the mechanosensitive transduction channel of vertebrate hair cells. *Nature* **432**: 723–730
- Correia MJ, Lang DG (1990) An electrophysiological comparison of solitary type I and type II vestibular hair cells. *Neurosci Lett* **116**: 106–111
- Coucke PJ, Hauwe PV, Kelley PM, Kunst H, Schatteman I, Velzen DV, Meyers J, Ensink RJ, Verstreken M, Declau F, Marres H, Kastury K, Bhasin S, McGuirt WT, Smith RJ, Cremers CW, Heyning PV, Willems PJ, Smith SD, Camp GV (1999) Mutations in the *KCNQ4* gene are responsible for autosomal dominant deafness in four DFNA2 families. *Hum Mol Genet* **8**: 1321–1328
- De Leenheer EM, Ensink RJ, Kunst HP, Marres HA, Talebizadeh Z, Declau F, Smith SD, Usami S, Van de Heyning PH, Van Camp G, Huygen PL, Cremers CW (2002) DFNA2/KCNQ4 and its manifestations. *Adv Otorhinolaryngol* **61**: 41–46
- Dechesne CJ, Rabejac D, Desmadryl G (1994) Development of calretinin immunoreactivity in the mouse inner ear. *J Comp Neurol* **346**: 517–529
- Devaux JJ, Kleopa KA, Cooper EC, Scherer SS (2004) KCNQ2 is a nodal K<sup>+</sup> channel. *J Neurosci* **24**: 1236–1244
- Gómez-Casati ME, Katz E, Glowatzki E, Lindudyno MI, Fuchs P, Elgoyhen AB (2004) Linopirdine blocks α9 α10-containing nicotinic cholinergic receptors of cochlear hair cells. *J Assoc Res Otolaryngol* **5**: 261–269
- Housley GD, Ashmore JF (1992) Ionic currents of outer hair cells isolated from the guinea-pig cochlea. *J Physiol* **448**: 73–98
- Jentsch TJ (2000) Neuronal KCNQ potassium channels: physiology and role in disease. *Nat Rev Neurosci* **1**: 21–30

- Kennedy HJ, Crawford AC, Fettiplace R (2005) Force generation by mammalian hair bundles supports a role in cochlear amplification. *Nature* **433**: 880–883
- Kharkovets T, Hardelin JP, Safieddine S, Schweizer M, El-Amraoui A, Petit C, Jentsch TJ (2000) KCNQ4, a K<sup>+</sup>-channel mutated in a form of dominant deafness, is expressed in the inner ear and in the central auditory pathway. *Proc Natl Acad Sci USA* **97**: 4333–4338
- Khimich D, Nouvian R, Pujol R, tom Dieck S, Egner A, Gundelfinger ED, Moser T (2005) Hair cell synaptic ribbons are essential for synchronous auditory signalling. *Nature* **434**: 889–894
- Kubisch C, Schroeder BC, Friedrich T, Lütjohann B, El-Amraoui A, Marlin S, Petit C, Jentsch TJ (1999) KCNQ4, a novel potassium channel expressed in sensory outer hair cells, is mutated in dominant deafness. *Cell* **96**: 437–446
- Lieberman MC, Gao J, He DZ, Wu X, Jia S, Zuo J (2002) Prestin is required for electromotility of the outer hair cell and for the cochlear amplifier. *Nature* **419**: 300–304
- Lindau M, Neher E (1988) Patch-clamp techniques for time-resolved capacitance measurements in single cells. *Pflügers Arch* **411**: 137–146
- Mammano F, Ashmore JF (1996) Differential expression of outer hair cell potassium currents in the isolated cochlea of the guinea-pig. *J Physiol* **496**: 639–646
- Marcotti W, Johnson SL, Holley MC, Kros CJ (2003) Developmental changes in the expression of potassium currents of embryonic, neonatal and mature mouse inner hair cells. *J Physiol* **548**: 383–400
- Marcotti W, Kros CJ (1999) Developmental expression of the potassium current  $I_{K,n}$  contributes to maturation of mouse outer hair cells. *J Physiol* **520**: 653–660
- Moser T, Beutner D (2000) Kinetics of exocytosis and endocytosis at the cochlear inner hair cell afferent synapse of the mouse. *Proc Natl Acad Sci USA* **97**: 883–888
- Nakagawa T, Kakehata S, Yamamoto T, Akaike N, Komune S, Uemura T (1994) Ionic properties of  $I_{K,n}$  in outer hair cells of guinea pig cochlea. *Brain Res* **661**: 293–297
- Neyroud N, Tesson F, Denjoy I, Leïbovici M, Donger C, Barhanin J, Faure S, Gary F, Coumel P, Petit C, Schwartz K, Guicheney P (1997) A novel mutation in the potassium channel gene *KVLQT1* causes the Jervell and Lange-Nielsen cardioauditory syndrome. *Nat Genet* **15**: 186–189
- Nouvian R, Ruel J, Guitton MJ, Pujol R, Puel JL (2003) Degeneration of sensory outer hair cells following pharmacological blockade of cochlear KCNQ channels in the adult guinea pig. *Eur J Neurosci* **17**: 2553–2562
- Oliver D, Knipper M, Derst C, Fakler B (2003) Resting potential and submembrane calcium concentration of inner hair cells in the isolated mouse cochlea are set by KCNQ-type potassium channels. *J Neurosci* **23**: 2141–2149
- Petit C, Levilliers J, Hardelin JP (2001) Molecular genetics of hearing loss. *Annu Rev Genet* **35**: 589–646
- Robles L, Ruggero MA (2001) Mechanics of the mammalian cochlea. *Physiol Rev* **81**: 1305–1352
- Rüttiger L, Sausbier M, Zimmermann U, Winter H, Braig C, Engel J, Knirsch M, Arntz C, Langer P, Hirt B, Müller M, Köpfschall I, Pfister M, Münkner S, Rohbock K, Pfaff I, Rüsch A, Ruth P, Knipper M (2004) Deletion of the Ca<sup>2+</sup>-activated potassium (BK)  $\alpha$ -subunit but not the BK  $\beta$ 1-subunit leads to progressive hearing loss. *Proc Natl Acad Sci USA* **101**: 12922–12927
- Ryan A, Dallos P (1975) Effect of absence of cochlear outer hair cells on behavioural auditory threshold. *Nature* **253**: 44–46
- Santos-Sacchi J, Huang GJ, Wu M (1997) Mapping the distribution of outer hair cell voltage-dependent conductances by electrical amputation. *Biophys J* **73**: 1424–1429
- Schmitt N, Schwarz M, Peretz A, Abitbol I, Attali B, Pongs O (2000) A recessive C-terminal Jervell and Lange-Nielsen mutation of the KCNQ1 channel impairs subunit assembly. *EMBO J* **19**: 332–340
- Schmitz F, Königstorfer A, Südhof TC (2000) RIBEYE, a component of synaptic ribbons: a protein's journey through evolution provides insight into synaptic ribbon function. *Neuron* **28**: 857–872
- Schroeder BC, Kubisch C, Stein V, Jentsch TJ (1998) Moderate loss of function of cyclic-AMP-modulated KCNQ2/KCNQ3 K<sup>+</sup> channels causes epilepsy. *Nature* **396**: 687–690
- Schwake M, Jentsch TJ, Friedrich T (2003) A carboxy-terminal domain determines the subunit specificity of KCNQ K<sup>+</sup> channel assembly. *EMBO Rep* **4**: 76–81
- Sobkowitz HM, Rose JE, Scott GE, Slapnick SM (1982) Ribbon synapses in the developing intact and cultured organ of Corti in the mouse. *J Neurosci* **2**: 942–957
- Sogaard R, Ljungstrom T, Pedersen KA, Olesen SP, Jensen BS (2001) KCNQ4 channels expressed in mammalian cells: functional characteristics and pharmacology. *Am J Physiol Cell Physiol* **280**: C859–C866
- Wang HS, Pan Z, Shi W, Brown BS, Wymore RS, Cohen IS, Dixon JE, McKinnon D (1998) KCNQ2 and KCNQ3 potassium channel subunits: molecular correlates of the M-channel. *Science* **282**: 1890–1893
- Weber T, Zimmermann U, Winter H, Mack A, Köpfschall I, Rohbock K, Zenner HP, Knipper M (2002) Thyroid hormone is a critical determinant for the regulation of the cochlear motor protein prestin. *Proc Natl Acad Sci USA* **99**: 2901–2906
- Yus-Najera E, Munoz A, Salvador N, Jensen BS, Rasmussen HB, Defelipe J, Villarroel A (2003) Localization of KCNQ5 in the normal and epileptic human temporal neocortex and hippocampal formation. *Neuroscience* **120**: 353–364
- Zenner HP, Reuter G, Zimmermann U, Gitter AH, Fermin C, LePage EL (1994) Transitory endolymph leakage induced hearing loss and tinnitus: depolarization, biphasic shortening and loss of electromotility of outer hair cells. *Eur Arch Otorhinolaryngol* **251**: 143–153
- Zheng J, Shen W, He DZ, Long KB, Madison LD, Dallos P (2000) Prestin is the motor protein of cochlear outer hair cells. *Nature* **405**: 149–155